Failure of Rubber Bearings Under Combined Shear and Compression

P. Mythravaruni
Faculty of Civil and Environmental Engineering,
Technion,
Haifa 3200003, Israel
e-mail: varuni.mythra@gmail.com

K. Y. Volokh
Faculty of Civil and Environmental Engineering,
Technion,
Haifa 3200003, Israel
e-mail: cvolokh@technion.ac.il

Rubber bearings, used for seismic isolation of structures, undergo large shear deformations during earthquakes as a result of the horizontal motion of the ground. However, the bearings are also compressed by the weight of the structure and possible traffic on it. Hence, failure analysis of rubber bearings should combine compression and shear. Such combination is considered in the present communication. In order to analyze failure, the strain energy density is enhanced with a limiter, which describes rubber damage. The inception of material instability and the onset of damage are marked by the violation of the condition of strong ellipticity, which is studied in the present work. Results of the studies suggest that horizontal cracks should appear because of the dominant shear deformation in accordance with the experimental observations. It is remarkable that compression delays failure in terms of the critical stretches.
[DOI: 10.1115/1.4040018]

1 Introduction

Rubber bearings are widely used in structural engineering yet the problem of their design is not completely resolved [1]. Among the difficulties, there is a necessity to understand and describe large deformations and failure of rubberlike materials. Thus, the purpose of this communication is to offer new approaches to attack the problem. The general idea is to analyze the onset of failure via the study of the violation of the condition of strong ellipticity under the prescribed shear-compression deformation.

We note that the traditional hyperelastic constitutive models are aimed at a description of the intact material behavior. In the latter case, various conditions are often imposed on the strain energy density functions in order to preclude material instability and provide the existence of the solution of a static boundary value problem. More physically appealing models should include a possibility and proper description of material failure. Few constitutive models developed in the past could capture the inception of material instability [2–6]. Interestingly, the material instability was observed in the mentioned works as an outcome of the specific and unintentional choice of the material models. Traditional systematic way to describe failure is based on continuum damage mechanics where internal damage variables are utilized in order to decrease and, ultimately, cancel material stiffness. The damage variable is described by an evolution equation and critical threshold condition [7–16]. While continuum damage mechanics is useful for considering gradual damage (e.g., Mullins effect), a much simpler framework without internal variables can describe the abrupt material failure [17]. This framework is based on the use of the limiting failure energy in the stored energy function. The limited stored energy automatically limits stresses defined by constitutive equations and it can be used for analysis of the onset of failure.

Recently, the approach of energy limiters was used for failure analyses, via the loss of strong ellipticity, in rubberlike materials under various deformations, including simple shear [18]. Evidently, the simple shear deformation is not enough for the consideration of mechanical behavior of rubber bearings in earthquakes. Combined compression-shear deformation should be considered. The latter is possible by using the deformation law proposed in Ref. [19]. For example, this law has been used for a calibration of very soft brain tissue [20]. Below, we use the compression-shear deformation law to perform failure analysis in rubber bearings.

2 Governing Equations

We refer to Ref. [21], for example, on the general background, and below, we briefly summarize the relevant generic equations and their specific forms.

The finite elasticity theory includes the equations of balance for linear and angular momenta in the reference configuration Ω_0

$$\begin{gathered}\rho_0 \partial^2 \mathbf{y}/\partial t^2 = \mathrm{Div}\mathbf{P} + \mathbf{b}_0 \\ \mathbf{P}\mathbf{F}^{\mathrm{T}} = \mathbf{F}\mathbf{P}^{\mathrm{T}}\end{gathered} \tag{1}$$

where ρ_0 is the mass density, $\mathbf{y}$ is the current position of material particle, "Div" is with respect to $\mathbf{x}$ designating the reference position of material particle, $\mathbf{b}_0$ is the body force, $\mathbf{P}$ is the first Piola–Kirchhoff stress, and $\mathbf{F} = \mathrm{Grad}\mathbf{y}$ is the deformation gradient.

For incompressible hyperelastic material, the stress is defined by

$$\mathbf{P} = \partial\psi/\partial\mathbf{F} - \Pi\mathbf{F}^{-\mathrm{T}}, \quad \det\mathbf{F} = 1 \tag{2}$$

where ψ is the density of the stored energy and Π is a Lagrange multiplier.

Natural or essential boundary conditions are defined on $\partial\Omega_0$

$$\mathbf{P}\mathbf{n}_0 = \bar{\mathbf{t}}_0 \quad \text{or} \quad \mathbf{y} = \bar{\mathbf{y}} \tag{3}$$

where $\mathbf{n}_0$ is an outward unit normal to $\partial\Omega_0$, $\bar{\mathbf{t}}_0$ is the given traction on $\partial\Omega_0$, $\mathbf{y}$ is related to $\mathbf{x}$ which is defined on $\partial\Omega_0$, and $\bar{\mathbf{y}}$ is prescribed.

Initial conditions are given in Ω_0 at $t = 0$

$$\mathbf{y} = \mathbf{y}_0, \quad \partial\mathbf{y}/\partial t = \mathbf{v}_0 \tag{4}$$

Introducing increments of all variables, designated with tildes, it is possible to set the corresponding incremental initial-boundary-value problem assuming the current configuration Ω as the referential one.

Skipping details of manipulations, the incremental momenta balance takes the form

$$\begin{gathered}\rho\partial^2\tilde{\mathbf{y}}/\partial t^2 = \mathrm{div}\tilde{\boldsymbol{\sigma}} \\ \tilde{\boldsymbol{\sigma}} + \boldsymbol{\sigma}\tilde{\mathbf{L}}^{\mathrm{T}} = (\tilde{\boldsymbol{\sigma}} + \boldsymbol{\sigma}\tilde{\mathbf{L}}^{\mathrm{T}})^{\mathrm{T}}\end{gathered} \tag{5}$$

where $\rho = \rho_0$, "div" is with respect to $\mathbf{y}$, $\boldsymbol{\sigma} = \mathbf{P}\mathbf{F}^{\mathrm{T}}$ is the Cauchy stress, $\tilde{\mathbf{L}} = \tilde{\mathbf{F}}\mathbf{F}^{-1}$, and $\tilde{\mathbf{F}} = \mathrm{Grad}\tilde{\mathbf{y}}$.

The incremental Cauchy stress is defined by the incremental constitutive law

$$\tilde{\boldsymbol{\sigma}} = \mathbb{A} : \tilde{\mathbf{L}} + \Pi\tilde{\mathbf{L}}^{\mathrm{T}} - \tilde{\Pi}\mathbf{1}, \quad \mathrm{tr}\tilde{\mathbf{L}} = 0, \tag{6}$$

where the elasticity tensor $\mathbb{A}$ has the following Cartesian components: $A_{ijkl} = F_{js}F_{lm}\partial^2\psi/\partial F_{is}\partial F_{km}$; and $\mathbf{1}$ is the identity tensor.

Contributed by the Applied Mechanics Division of ASME for publication in the Journal of Applied Mechanics. Manuscript received March 8, 2018; final manuscript received April 17, 2018; published online May 15, 2018. Assoc. Editor: Shaoxing Qu.

We assume that external loads and given surface positions of material points do not depend on deformation (dead) and we can write the incremental boundary conditions on $\partial\Omega$

$$\tilde{\boldsymbol{\sigma}}\mathbf{n} = \mathbf{0} \quad \text{or} \quad \tilde{\mathbf{y}} = \mathbf{0} \tag{7}$$

where $\mathbf{n} = |\mathbf{F}^{-\mathrm{T}}\mathbf{n}_0|^{-1}\mathbf{F}^{-\mathrm{T}}\mathbf{n}_0$ is a unit outward normal to $\partial\Omega$.

The initial conditions in Ω are

$$\tilde{\mathbf{y}} = \mathbf{0}, \quad \partial\tilde{\mathbf{y}}/\partial t = \mathbf{0} \tag{8}$$

If the strain energy $\psi(I_1)$ depends on the first principal invariant $I_1 = \mathbf{F} : \mathbf{F}$ only, then we have

$$A_{ijkl} = 4\psi_{11}F_{is}F_{km}F_{js}F_{lm} + 2\psi_1\delta_{ki}F_{jm}F_{lm} \tag{9}$$

where $\psi_1 \equiv \partial\psi/\partial I_1$ and $\psi_{11} \equiv \partial\psi_1/\partial I_1$.

A plane wave solution of the incremental equations (5) is considered

$$\tilde{\mathbf{y}} = \mathbf{k}g(\mathbf{m}\cdot\mathbf{y} - wt), \quad \tilde{\Pi} = \Upsilon g'(\mathbf{m}\cdot\mathbf{y} - wt) \tag{10}$$

in which $\mathbf{k}$, $\mathbf{m}$, and w are polarization, direction, and speed of the wave accordingly, prime is derivative with respect to the argument of g, and Υ is the amplitude of the increment of the Lagrange multiplier.

Substituting the solution in the incremental equations (5), we get

$$\rho w^2\mathbf{k} = \boldsymbol{\Lambda}\mathbf{k} - \Upsilon\mathbf{m}, \quad \mathbf{k}\cdot\mathbf{m} = 0 \tag{11}$$

where $\boldsymbol{\Lambda}$ is the acoustic tensor with components $\Lambda_{mi} = A_{mnij}m_n m_j$.

Calculating the dot product of $(11)_1$ with $\mathbf{m}$, we can get Υ and, consequently, rewrite (11) in the form

$$\rho w^2\mathbf{k} = \boldsymbol{\Lambda}^*\mathbf{k}, \quad \mathbf{k}\cdot\mathbf{m} = 0 \tag{12}$$

where $\boldsymbol{\Lambda}^* = \boldsymbol{\Lambda} - \mathbf{m}\otimes\boldsymbol{\Lambda}\mathbf{m}$ designates acoustic tensor for incompressible material.

Note that $\boldsymbol{\Lambda}^{*\mathrm{T}}\mathbf{m} = \mathbf{0}$ and, consequently, $\boldsymbol{\Lambda}^*$ is singular the left eigenvector $\mathbf{m}$ corresponding to zero eigenvalue. Thus, no more than two real waves exist which are transverse due to incompressibility $(12)_2$. Calculating the dot product of $(11)_1$ with $\mathbf{k}$ gives the wave speed obeying the condition of strong ellipticity

$$\rho w^2 = \mathbf{k}\cdot\boldsymbol{\Lambda}\mathbf{k} > 0 \tag{13}$$

If the strain energy ψ depends on I_1 only, then the acoustic tensor is simple

$$\boldsymbol{\Lambda} = 4\psi_{11}(\mathbf{Bm})\otimes(\mathbf{Bm}) + 2\psi_1(\mathbf{m}\cdot\mathbf{Bm})\mathbf{1} \tag{14}$$

in which the left Cauchy–Green tensor $\mathbf{B} = \mathbf{F}\mathbf{F}^{\mathrm{T}}$ is used.

In this particular case, the wave speed is calculated as

$$\rho w^2 = 4\psi_{11}(\mathbf{k}\cdot\mathbf{Bm})^2 + 2\psi_1(\mathbf{m}\cdot\mathbf{Bm}) \tag{15}$$

Finally, we specify the strain energy including a material failure description in the form

$$\psi(\mathbf{F},\zeta) = \psi_{\mathrm{f}} - H(\zeta)\psi_{\mathrm{e}}(\mathbf{F}) \tag{16}$$

where

$$\psi_{\mathrm{e}}(\mathbf{F}) = \Phi m^{-1}\Gamma(m^{-1}, W(\mathbf{F})^m\Phi^{-m}), \quad \psi_{\mathrm{f}} = \psi_{\mathrm{e}}(\mathbf{1}) \tag{17}$$

and

$$\Gamma(s,x) = \int_x^\infty t^{s-1}e^{-t}dt$$

is the upper incomplete gamma function.

Here, we designated failure energy ψ_{f} and elastic energy $\psi_{\mathrm{e}}(\mathbf{F})$. Material healing is prevented by the step function: $H(\zeta) = 0$ if $\zeta < 0$ or $H(\zeta) = 1$ otherwise. The stored energy without failure is designated by $W(\mathbf{F})$, while Φ is the energy limiter and m is a material parameter.

We note that $\zeta \in (-\infty, 0]$ is calculated from the evolution equation

$$\dot{\zeta} = -H(\epsilon - \psi_{\mathrm{e}}/\psi_{\mathrm{f}}), \quad \zeta(0) = 0 \tag{18}$$

in which $0 < \epsilon \ll 1$ is a precision limit.

According to Eq. (16), deformation is reversible as long as ψ is less than ψ_{f}. The strain energy stays fixed after reaching this limit and, hence, the deformation becomes irreversible. Note that ζ is a switch function rather than internal variable: if $\zeta = 0$, then the deformation is hyperelastic, and if $\zeta < 0$, then the deformation is irreversible.

Constitutive law is derived from Eq. (16) by using a thermodynamic reasoning [22]

$$\mathbf{P} = -H(\zeta)\partial\psi_{\mathrm{e}}(\mathbf{F})/\partial\mathbf{F} \tag{19}$$

The reader should notice that in the cases where material unloading is not relevant, we can set $\zeta \equiv 0 \Rightarrow H(\zeta) \equiv 1$. The latter simplification is done in the present work.

3 Compression Combined With Shear in Rubber Bearings

Following Ref. [19], we define the compression-shear deformation law as

$$y_1 = \lambda^{-1/2}x_1 + \lambda\gamma x_2, \quad y_2 = \lambda x_2, \quad y_3 = \lambda^{-1/2}x_3 \tag{20}$$

and, consequently, we calculate

$$\begin{aligned}
\mathbf{F} &= \lambda^{-1/2}\mathbf{e}_1\otimes\mathbf{e}_1 + \lambda\gamma\mathbf{e}_1\otimes\mathbf{e}_2 + \lambda\mathbf{e}_2\otimes\mathbf{e}_2 + \lambda^{-1/2}\mathbf{e}_3\otimes\mathbf{e}_3,\\
\mathbf{B} &= (\lambda^{-1} + \lambda^2\gamma^2)\mathbf{e}_1\otimes\mathbf{e}_1 + \lambda^2\gamma\mathbf{e}_1\otimes\mathbf{e}_2 + \lambda^2\gamma\mathbf{e}_2\otimes\mathbf{e}_1\\
&\quad + \lambda^2\mathbf{e}_2\otimes\mathbf{e}_2 + \lambda^{-1}\mathbf{e}_3\otimes\mathbf{e}_3
\end{aligned} \tag{21}$$

where $\mathbf{e}_1, \mathbf{e}_2, \mathbf{e}_3$ are Cartesian basis vectors, λ is the axial stretch, and γ is the amount of shear.

Specific forms of the unit vectors in the directions of wave propagation and wave polarization are chosen as follows:

$$\begin{aligned}
\mathbf{m} &= \cos\alpha\mathbf{e}_1 + \sin\alpha\mathbf{e}_2,\\
\mathbf{k} &= -\beta\sin\alpha\mathbf{e}_1 + \beta\cos\alpha\mathbf{e}_2 + \sqrt{1-\beta^2}\mathbf{e}_3
\end{aligned} \tag{22}$$

where α is the angle in plane $x_1 - x_2$ and $0 \le \beta \le 1$ is an arbitrary multiplier.

Then, we have

$$\begin{aligned}
\mathbf{Bm} &= (\cos\alpha(\lambda^{-1} + \lambda^2\gamma^2) + \gamma\lambda^2\sin\alpha)\mathbf{e}_1\\
&\quad + (\lambda^2\gamma\cos\alpha + \lambda^2\sin\alpha)\mathbf{e}_2,\\
\mathbf{m}\cdot\mathbf{Bm} &= \cos^2\alpha(\lambda^{-1} + \lambda^2\gamma^2) + \gamma\lambda^2\sin(2\alpha) + \lambda^2\sin^2\alpha,\\
\mathbf{k}\cdot\mathbf{Bm} &= \beta\sin(2\alpha)(\lambda^2 - \lambda^{-1} - \lambda^2\gamma^2)/2 + \beta\gamma\lambda^2\cos(2\alpha)
\end{aligned} \tag{23}$$

and, consequently, the weighted squared wave speed (15) can be expressed as

$$\begin{aligned}
\rho w^2 &= 4\psi_{11}(\beta\sin(2\alpha)(\lambda^2 - \lambda^{-1} - \lambda^2\gamma^2)/2 + \beta\gamma\lambda^2\cos(2\alpha))^2\\
&\quad + 2\psi_1(\cos^2\alpha(\lambda^{-1} + \lambda^2\gamma^2) + \gamma\lambda^2\sin(2\alpha) + \lambda^2\sin^2\alpha)
\end{aligned} \tag{24}$$

Table 1 Material constants for the natural rubber vulcanizate

c_1 (MPa)	c_2 (MPa)	c_3 (MPa)	Φ (MPa)	m
0.298	0.014	0.00016	82	10

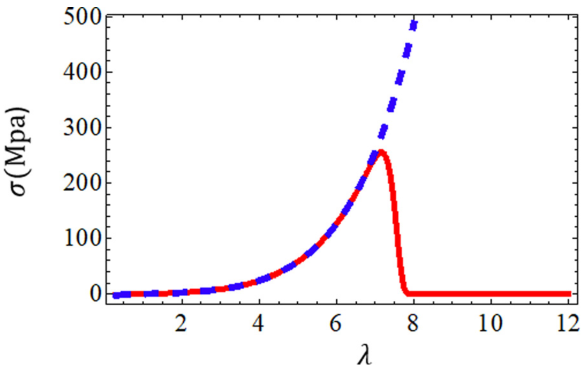

Fig. 1 Cauchy stress versus stretch for uniaxial tension. Dashed line is for the model without failure and solid line is for the model with failure.

Then, we obtain from Eq. (16) ($H \equiv 1$)

$$\psi_1 = W_1 \exp[-W^m \Phi^{-m}],$$
$$\psi_{11} = (W_{11} - mW^{m-1}\Phi^{-m}W_1^2)\exp[-W^m\Phi^{-m}] \quad (25)$$

where we use the Yeoh stored energy function

$$W = c_1(I_1 - 3) + c_2(I_1 - 3)^2 + c_3(I_1 - 3)^3,$$
$$W_1 = c_1 + 2c_2(I_1 - 3) + 3c_3(I_1 - 3)^2, \quad (26)$$
$$W_{11} = 2c_2 + 6c_3(I_1 - 3)$$

with $I_1 = \lambda^2(1 + \gamma^2) + 2/\lambda$.

Material constants for this model were calibrated in one-, two- and three-dimensional stress–strain states [21] for natural rubber vulcanizate—see Table 1.

For the sake of illustration, the stress–strain curve for the considered model is shown in Fig. 1.

Material instability sets in when the wave speed is zero

$$\rho w^2 = f_1 f_2 = 0 \quad (27)$$

where

$$f_1 = 4(W_{11} - mW^{m-1}\Phi^{-m}W_1^2)(\beta \sin(2\alpha)(\lambda^2 - \lambda^{-1} - \lambda^2\gamma^2)/2 + \cos(2\alpha)\beta\gamma\lambda^2)^2 + 2W_1(\cos^2\alpha(\lambda^{-1} + \lambda^2\gamma^2) + \gamma\lambda^2 \sin(2\alpha) + \lambda^2 \sin^2\alpha),$$
$$f_2 = \exp[-W^m\Phi^{-m}] \quad (28)$$

The split conditions read

$$f_1 = 0, \quad f_2 = 0 \quad (29)$$

Function f_2 depending on amount of shear is shown graphically in Fig. 2 for various amounts of compression.

The reader should note the numerical convergence to zero, which means that the theoretical "infinity" very fast becomes the digital one.

Hence, the critical conditions get the graphical representation in terms of two curves depending on α, β, γ, and λ—Fig. 3.

The reader should note that f_2 does not depend on α and β, while for f_1 the magnitude of γ increases with the decreasing β for

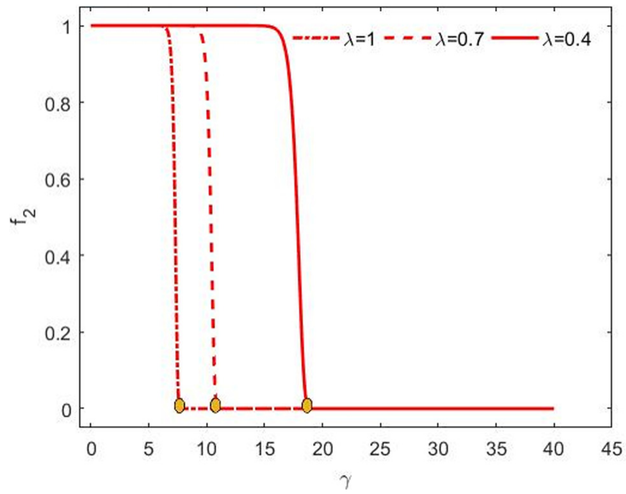

Fig. 2 Convergence of $f_2(\gamma)$ to zero for various amounts of compression

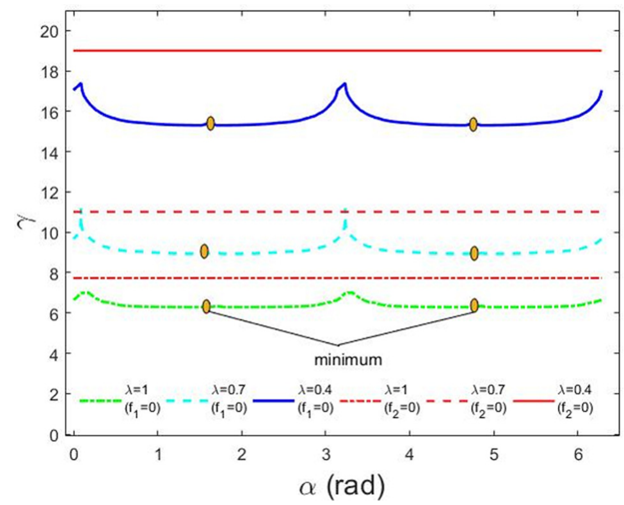

Fig. 3 Shear versus the orientation of the superposed acoustic wave. Curves $f_1 = 0$ ($\beta = 1$) and $f_2 = 0$ are presented for various values of compression stretch. The minimum shear indicates the inception of instability through the loss of strong ellipticity.

all compression stretches. The lowest amount of shear is always obtained for $\alpha = \pi/2$ (or $\alpha = 3\pi/2$), which can be interpreted as localization of failure along axis x_1 and, consequently, *the crack should appear in the horizontal direction*. Remarkably, the on-site observation shown in Photo 3 of paper [23] perfectly confirms the theoretical prediction.

It is also remarkable that the increase of compression (decrease of stretch) leads to the increase of the critical amount of shear corresponding to failure. In other words, compression delays failure. Physically, the latter fact can be explained as follows. Failure in shear is triggered by huge tension of material filaments,[1] which were vertical before deformation. Compression delays transition of the filaments to tension, including the critical tension. Of course, such explanation is not absolute and the game of strains is more sophisticated. Nevertheless, the explanation might give some intuition concerning the deformation and failure process.

Finally, it is interesting to see the correlation between the loss of strong ellipticity and the material strength in shear—Fig. 4.

[1]By filaments, we mean the aligned collections of material points following the continuum mechanics approach in which real physical particles are replaced (averaged) by the abstract material points (representative volumes).

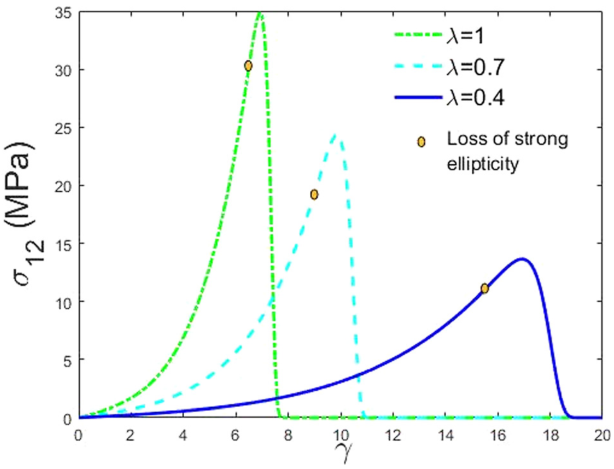

Fig. 4 Shear stress versus amount of shear for various values of compression. Limit points designate the material strength and the elliptical markers on the curves indicate the loss of the strong ellipticity.

The diagrams show the dependence of the Cauchy shear stress on the amount of shear. The limit points indicate the strength, while the elliptical markers on the curves indicate the loss of the strong ellipticity.

4 Conclusion

In this note, we analyzed failure of rubber bearings under combined shear and compression. We included a failure description in the constitutive model via an energy limiter. This model had been calibrated for a natural rubber vulcanizate under various stress–strain states. The onset of failure was associated with the loss of the strong ellipticity for the incremental boundary-value problem. We found that the failure should localize into cracks in the direction of shear—the horizontal direction. The latter prediction was in perfect qualitative agreement with the on-site observations. We also found that the superimposed compression delayed the onset of the critical failure stretches, which would be good from the structural design standpoint.

Funding Data

- Israel Science Foundation (ISF 198/15).

References

[1] Gent, A. N., 2001, *Engineering With Rubber*, 2nd ed., Hanser, Munich, Germany.

[2] Kurashige, M., 1981, "Instability of a Transversely Isotropic Elastic Slab Subjected to Axial Loads," ASME J. Appl. Mech., **48**(2), pp. 351–356.

[3] Triantafyllidis, N., and Abeyaratne, R., 1983, "Instability of a Finitely Deformed Fiber-Reinforced Elastic Material," ASME J. Appl. Mech., **50**(1), pp. 149–156.

[4] Danescu, A., 1991, "Bifurcation in the Traction Problem for a Transversely Isotropic Material," Math. Proc. Camb. Philos. Soc., **110**(2), pp. 385–394.

[5] Merodio, J., and Ogden, R. W., 2002, "Material Instabilities in Fiber-Reinforced Nonlinearly Elastic Solids Under Plane Deformation," Arc. Mech., **54**(5–6), pp. 525–552.

[6] Dorfmann, L., and Ogden, R. W., eds., 2015, *Nonlinear Mechanics of Soft Fibrous Materials*, Springer, Wien, Austria.

[7] Simo, J. C., 1987, "On a Fully Three-Dimensional Finite Strain Viscoelastic Damage Model: Formulation and Computational Aspects," Comp. Meth. Appl. Mech. Eng., **60**(2), pp. 153–173.

[8] Govindjee, S., and Simo, J. C., 1991, "A Micro-Mechanically Based Continuum Damage Model of Carbon Black-Filled Rubbers Incorporating the Mullins Effect," J. Mech. Phys. Solids, **39**(1), pp. 87–112.

[9] Johnson, M. A., and Beatty, M. F., 1993, "A Constitutive Equation for the Mullins Effect in Stress Controlled in Uniaxial Extension Experiments," Cont. Mech. Therm., **5**(4), pp. 301–318.

[10] Miehe, C., 1995, "Discontinuous and Continuous Damage Evolution in Ogden-Type Large-Strain Elastic Materials," Eur. J. Mech. A, **14**(5), pp. 697–720.

[11] De Souza Neto, E. A., Peric, D., and Owen, D. R. J., 1998, "Continuum Modeling and Numerical Simulation of Material Damage at Finite Strains," Arch. Comp. Meth. Eng., **5**(4), pp. 311–384.

[12] Ogden, R. W., and Roxburgh, D. G., 1999, "A Pseudo-Elastic Model for the Mullins Effect in Filled Rubber," Proc. Roy. Soc. London Ser. A, **455**(1988), pp. 2861–2877.

[13] Menzel, A., and Steinmann, P., 2001, "A Theoretical and Computational Framework for Anisotropic Continuum Damage Mechanics at Large Strains," Int. J. Solids Struct., **38**(52), pp. 9505–9523.

[14] Guo, Z., and Sluys, L., 2006, "Computational Modeling of the Stress-Softening Phenomenon of Rubber Like Materilas Under Cyclic Loading," Eur. J. Mech. A, **25**(6), pp. 877–896.

[15] De Tommasi, D., Puglisi, G., and Saccomandi, G., 2008, "Localized Vs Diffuse Damage in Amorphous Materials," Phys. Rev. Lett., **100**(8), p. 085502.

[16] Dal, H., and Kaliske, M., 2009, "A Micro-Continuum-Mechanical Material Model for Failure of Rubberlike Materials: Application to Ageing-Induced Fracturing," J. Mech. Phys. Solids, **57**(8), pp. 1340–1356.

[17] Volokh, K. Y., 2013, "Review of the Energy Limiters Approach to Modeling Failure of Rubber," Rubber. Chem. Technol., **86**(3), pp. 470–487.

[18] Volokh, K. Y., 2017, "Loss of Ellipticity in Elasticity With Energy Limiters," Eur. J. Mech. A, **63**, pp. 36–42.

[19] Rajagopal, K. R., and Wineman, A. S., 1987, "New Universal Relations for Nonlinear Isotropic Elastic Materials," J. Elast., **17**(1), pp. 75–83.

[20] Mihai, L. A., Budday, S., Holzapfel, G. A., Kuhl, E., and Goriely, A., 2017, "A Family of Hyperelastic Models for Human Brain Tissue," J. Mech. Phys. Solids, **106**, pp. 60–79.

[21] Volokh, K. Y., 2016, *Mechanics of Soft Materials*, Springer, Singapore.

[22] Volokh, K. Y., 2014, "On Irreversibility and Dissipation in Hyperelasticity With Softening," ASME J. Appl. Mech., **81**(7), p. 074501.

[23] Takahashi, Y., 2012, "Damage of Rubber Bearings and Dambers of Bridges in 2011 Great East Japan Earthquake," International Symposium on Engineering Lessons Learned From the 2011 Great East Japan Earthquake, Tokyo, Japan, Mar. 1–4, pp. 1333–1342.